Notes

X-Band ENDOR of the Liganding Environment from the Radical X Intermediate of *Escherichia coli* Ribonucleotide Reductase

Andrei Veselov and Charles P. Scholes*

Department of Chemistry, University at Albany, State University of New York, Albany, New York 12222

Received December 5, 1995

Introduction

Ribonucleotide reductase (RNR) catalyzes the formation of deoxyribonucleotides from ribonucleotides as a precursor to DNA synthesis. The diiron center of its smaller subunit, R2, activates O_2 and facilitates formation of a stable tyrosine radical (•Y122); the diiron cofactor and the tyrosyl radical are required for nucleotide reduction.[1a,b] In the resting enzyme the diferric center is antiferromagnetically coupled and EPR silent; X-ray crystallography shows that each iron has one water ligand and one histidine ligand.[1a,b] In cofactor assembly from apoprotein and ferrous ion in the presence of dioxygen, an observable, kinetically competent diiron ($S = {}^1/_2$) species, Intermediate X, arises. An interpretation of freeze−quench EPR and Mössbauer is that this intermediate arises from two high spin ($S = {}^5/_2$) ferric ions coupled to a third radical spin ($S = {}^1/_2$) to give the overall $S = {}^1/_2$ diferric radical, Intermediate X species.[2a−f] Calculations in ref 2f have suggested that the coupled radical is an oxyl (•O^-) radical that bridges the two irons.

The dinuclear cluster found in R2 has a catalytic motif similar to that in functionally quite different proteins, notably, hemerythrin[3a] (Hr), which reversibly binds O_2, and methane monooxygenase[3b] (MMO), which activates O_2 for oxidation of hydrocarbon substrates. The diiron cofactors of MMO and Hr can also be prepared in paramagnetic, partially reduced, mixed-valent or semimet ($S = {}^1/_2$) forms, but in contrast to Intermediate X, the coupling scheme which accounts for their $S = {}^1/_2$ ground state and intimately influences their EPR signal is antiferromagnetic coupling between their ferric ($S = {}^5/_2$) and ferrous ($S = 2$) irons. From both semimet Hr[4b,c] and mixed-valent MMO[4a−c] there is ENDOR evidence of exchangeable protons, possibly attached to a bridging oxygen, and of nitrogen ligand(s) to the iron centers. This note provides corresponding evidence from Intermediate X for its exchangeable proton and nitrogen couplings.

Experimental Section

Methods. X-band ENDOR was performed under dispersion, rapid passage conditions on a home-built spectrometer[5] at pumped liquid helium temperature ($T = 2.1$ K). Noise broadening of the ENDOR rf (radio frequency) source[6] or chopping of the rf with a 10% duty cycle having 10 μs rf pulses of 8 W intensity led to ENDOR features with higher signal-to-noise. Large field modulation of order 5 G ptp (peak to peak) succeeded in better bringing in large couplings to exchangeable protons[7] and also to nitrogens.

Materials. Preparation of Intermediate X for ENDOR spectroscopy was carried out by modifications of rapid freeze−quench procedures previously described.[8] An oxygen-saturated solution of apo-Y122F/Y356F (357 μM) in 100 mM HEPES, pH 7.7, was transferred to the drive syringe of an Update Instruments System 1000. A solution of $FeSO_4$ (1.79 mM in 5 mN H_2SO_4) was saturated with oxygen gas and transferred to the second drive syringe. The reaction was initiated by mixing equal volumes of these solutions at 5 °C and quenching at 428 ms into an ENDOR tube. Taking care to insure equality between the pD and the pH of the corresponding protonated sample, we performed experiments with D_2O in similar fashion.[9] Parts A (protonated solvent) and B (deuterated solvent) of Figure 1 show the EPR signals of Intermediate X obtained from R2-Y122F/Y356F. The protonated spectrum shown in Figure 1A is identical to that obtained previously from the diferric radical of the single mutant R2-Y122F (ref 1c, Figure 6A). Since it reflects loss of hyperfine couplings to exchangeable protons, the deuterated spectrum shown in Figure 1B is slightly narrower than the protonated spectrum shown in Figure 1A. A small g anisotropy has been reported ($g_{\|} = 2.006$, $g_{\perp} = 1.994$)[2c] in the X-band EPR spectrum of Intermediate X, and accordingly in Figure 1, the positive lobe of the absorption derivative EPR signal below the line center was slightly broader than the negative lobe above the line center.

The construction and expression of R2-Y122F/Y356F was carried out in the following manner: The mutant R2-Y122F/Y356F was made using the polymerase chain reaction (PCR) method described by Ho.[10] Degenerate primers for the PCR reactions were designed from the known sequence of pTB2 (containing the coding sequence of R2) and engineered with restriction sites to facilitate cloning of the amplified fragments. The amplified products were purified on an agarose gel in TAE buffer, and the resulting fragment was ligated into the expression vector pTB2. This mutant plasmid was used to transform *Escherichia coli* K38 containing pGP1-2. Protein was overexpressed and isolated from cells resistant to both ampicillin and kanamycin. The mutation of tyrosines 122 and 356 to the less easily oxidized phenylalanine results in a nearly stoichiometric accumulation of Intermediate X and removes the potential for spectral interference from tyrosine radicals.

Results and Discussion

Proton ENDOR. A large, clearly exchangeable proton feature labeled "Ex" appeared from the protonated samples with ENDOR frequencies in the 22−25 MHz region (Figure 2A,B)

* To whom correspondence should be addressed.

(1) (a) Nordlund, P.; Sjöberg, B.-M.; Eklund, H. *Nature* **1990**, *345*, 593−598. (b) Nordlund, P.; Eklund, H. *J. Mol. Biol.* **1993**, 232, 123−164.
(2) (a) Bollinger, J. M., Jr.; Stubbe, J.; Huynh, B. H.; Edmondson, D. E. *J. Am. Chem. Soc.* **1991**, *113*, 6289−6291. (b) Bollinger, J. M.; Edmondson, D. E.; Huynh, B. H.; Filley, J.; Norton, J. R.; Stubbe, J. *Science* **1991**, *253*, 292−298. (c) Ravi, N.; Bollinger, J. M.; Huynh, B. H.; Edmondson, D. E.; Stubbe, J. *J. Am. Chem. Soc.* **1994**, *116*, 8007−8014. (d) Bollinger, J. M., Jr.; Wing, H. T.; Ravi, N.; Huynh, B. H.; Edmondson, D. E.; Stubbe, J. *J. Am.Chem. Soc.* **1994**, *116*, 8015−8023. (e) Bollinger, J. M., Jr.; Wing, H. T.; Ravi, N.; Huynh, B. H.; Edmondson, D. E.; Stubbe, J. *J. Am. Chem. Soc.* **1994**, *116*, 8024−8032. (f) Ravi, N.; Bominaar, E. L. *Inorg. Chem.* **1995**, *34*, 1040−1043.
(3) (a) Scheriff, S.; Hendrickson, W. A.; Smith, J. L. *J. Mol. Biol.* **1987**, *197*, 273−296. (b) Rosenzweig, A. C.; Frederick, C. A.; Lippard, S. J.; Nordlund, P. *Nature* **1993**, *366*, 537−543.
(4) (a) Hendrich, M. P.; Fox, B. G.; Andersson, K. K.; DeBrunner, P. G.; Lipscomb, J. D. *J. Biol. Chem.* **1992**, *267*, 261−269. (b) DeRose, V. J.; Liu, K. E.; Kurtz, D. M.; Hoffman, B. M.; Lippard, S. J. *J. Am. Chem. Soc.* **1993**, *115*, 6440−6441. (c) Thomann, H.; Bernardo, M.; McCormick, J. M.; Pulver, S.; Andersson, K. K.; Lipscomb, J. D.; Solomon, E. I. *J. Am. Chem. Soc.* **1993**, *115*, 8881−8882.
(5) Scholes, C. P.; Falkowski, K. M.; Chen, S.; Bank, J. F. *J. Am. Chem. Soc.* **1986**, *108*, 1660−1671.
(6) Hoffman, B. M.; DeRose, V. J.; Ong, J. L.; Davoust, C. E. *J. Magn. Reson.* **1994**, *110*, 52−57.
(7) (a) Tan, X-L.; Bernardo, M.; Thomann, M.; Scholes, C. P. *J. Chem. Phys.* **1993**, *98*, 5147−5157. (b)Tan, X.-L.; Bernardo, M.; Thomann, M.; Scholes, C. P. *J. Chem. Phys.* **1995**, 102, 2675−2690.
(8) Bollinger, M. J., Jr.; Tong, W. H.; Huynh, B. H.; Edmondson, D. E.; Stubbe, J. *Methods Enzym.*, in press.
(9) Glasoe, P. K.; Long, F. A. *J. Chem Soc. A* **1960**, 188.
(10) Ho, S. N.; Hunt, H. D.; Horton, R. M.; Pullen, J. K.; Pease, L. R. *Gene* **1989**, *77*, 51−59.

S0020-1669(95)01544-8 CCC: $12.00

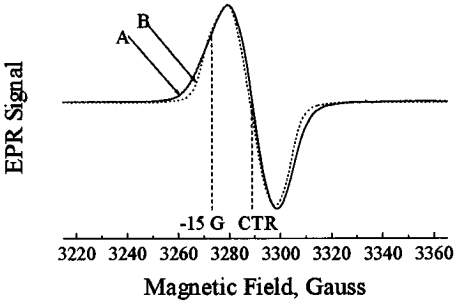

Figure 1. Comparison of the EPR spectra of Intermediate X in protonated and in deuterated solvent. Experimental conditions were T = 4.2 K, microwave power ~ 0.6 μW, modulation ~ 3 G ptp, experimental time constant 0.1 s. Spectrum A is from the sample prepared with protonated solvent, and its EPR frequency was 9.1975 GHz. Spectrum B is from the sample prepared with deuterated solvent; its EPR frequency was 9.2049 GHz, and Spectrum B was shifted 1.7 G to lower field to account for the EPR frequency difference from 9.1975 GHz. The g value at the EPR line center was 1.998, and that at 15 G below the line center was 2.007.

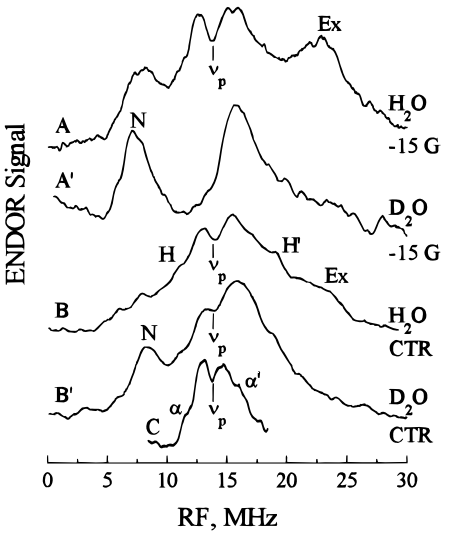

Figure 2. ENDOR spectra taken in the 1−31 MHz range from protonated (A,B) and deuterated (A′,B′) samples to show couplings to proton and nitrogen features. Features labeled "Ex" are from strongly coupled, exchangeable protons. Features labeled "N" are those assigned to nitrogen. ν_p is the position of the proton Larmor frequency. A. Spectrum from protonated sample taken 15 G below the EPR line center under the following conditions: rf power = 0.3 W, microwave power ~ 0.5 μW, field modulation ~ 3 G ptp, rf noise broadening of approximately 100 KHz width, and 138 data accumulations of 10 s each at sweep rate of 3 MHz/s and system time constant 0.1 s. A′. Spectrum from deuterated sample taken 15 G below the EPR line center under the following conditions: rf power = 0.75 W, microwave power ~ 0.5 μW, field modulation ~ 3 G ptp, rf noise broadening of approximately 100 KHz width, and 946 data accumulations of 20 s each at sweep rate of 1.5 MHz/s and system time constant 0.1 s. At this position on the EPR line for the deuterated sample the "dip" near the free proton frequency was not as obvious as in the spectra A, B, and B′. B. Spectrum from protonated sample taken at the EPR line center under conditions of spectrum 2A; the number of data accumulations was 65. B′. Spectrum from deuterated sample taken at the EPR line center under conditions of spectrum 2A; the number of data accumulations was 128. C. Spectrum taken from deuterated sample 5 G below the EPR line center under the following conditions: rf power = 0.75 W, microwave power ~ 0.5 μW, field modulation ~ 0.3 G ptp, rf noise broadening of approximately 100 KHz width, and 55 data accumulations of 5 s each at sweep rate of 2 MHz/s and system time constant 0.05 s.

but not the deuterated (Figure 2A′,B′). The hyperfine coupling to that exchangeable feature, as calculated by the usual first-order approximation (see below), was ~18.5 MHz at the peak in Figure 2A, and the coupling at the high frequency edge was ~23 MHz. There was a sharper appearance of the exchangeable ENDOR peak in Figure 2A taken 15 G to the low field ($g_{\|}$) side of the EPR spectrum. The exchangeable feature in the 22−25 MHz region was well detected at all g values between $g_{\|}$ and $g_{\perp}$. It became broadened and less intense as it approached the central $g_{\perp}$ region, and it became impossible to detect to the high field side of $g_{\perp}$. Additional weakly resolved exchangeable proton features, H,H′, were observed with splitting of about 8 MHz. There were broad features within ~±2 MHz of the proton Larmor frequency that were altered or attenuated by deuterium exchange. In the deuterated sample a frequency sweep with small field modulation amplitude over a narrow frequency range near ν_p (Figure 2C) revealed a set of weakly resolved shoulders, α,α′, with splitting of 4.5 MHz. The feature near 17 MHz in Figure 2A′ did not disappear on deuteration because this feature was a nonexchangeable proton feature whose partner below the free proton frequency was diminished by the fast rf frequency sweep under rapid passage conditions.

For protons the first-order ENDOR frequencies are $^{H}\nu^{+} = |\nu_p + {}^{H}A/2|$ and $^{H}\nu^{-} = |\nu_p - {}^{H}A/2|$, where ^{H}A is the electron proton hyperfine coupling. Ideally a pair of proton features is expected to be centered at the free proton frequency, $\nu_p = 14$ MHz, and separated from each other by ^{H}A. In instances when the hyperfine coupling is comparable to the nuclear Zeeman frequency, the ν^{+} branch is often more intense than the ν^{-} branch, as described in ref 15. First-order theory works best when there is colinearity of the magnetic field and a principle electron−nuclear hyperfine axis. For frozen solution samples, those g values where there is colinearity yield more intense and better resolved ENDOR features, like the exchangeable feature in Figure 2A. In the most general case when the hyperfine interaction is comparable to the Zeeman interaction and the hyperfine and **g**-tensors are highly anisotropic, more elaborate ENDOR features not centered at ν_p may arise, and multiple extremal turning points in the ENDOR spectra of frozen solutions may occur.[14] Nevertheless, when the **g** tensor is only slightly anisotropic, there will be orientations where an absolute maximum in hyperfine coupling is measured and where the nuclear Zeeman and hyperfine interactions are colinear.[14] Here that absolute maximum hyperfine coupling for the exchangeable protons is greater than 18 MHz.

The net hyperfine tensor, **A**, of a nucleus in the vicinity of diferric Intermediate X would be the sum of its tensor contributions from the spin centers which make up the diferric radical. Following eq 6 of ref 2c,

$$\mathbf{A} = 2.161\mathbf{A}_{\mathrm{Fe_{(III)2}}} - 1.126\mathbf{A}_{\mathrm{Fe_{(III)1}}} - 0.035\mathbf{A}_{\mathrm{radical}} \qquad (1)$$

where $\mathbf{A}_{\mathrm{Fe_{(III)2}}}$, $\mathbf{A}_{\mathrm{Fe_{(III)1}}}$, and $\mathbf{A}_{\mathrm{radical}}$ are the individual intrinsic hyperfine tensors for the nucleus in question as it interacts with electron spin on $\mathrm{Fe_{(III)2}}$, $\mathrm{Fe_{(III)1}}$, and the coupled radical, respectively.[11] $\mathrm{Fe_{(III)2}}$ (Fe site 2) is the iron with the larger, positive hyperfine coupling in the diferric radical.[2c,d] ($\mathrm{Fe_{(III)2}}$ has been speculated[2c] as the iron that in the resting, antiferrromagnetically coupled diferric enzyme is coordinated in bidentate fashion by aspartate 84[1b] and is the closer of the two irons to the •Y122 radical.) When the observed proton is a simple terminal proton attached to only one iron, an axial hyperfine

(11) For mixed-valence MMO and semimet Hr, the coefficients of the Fe(III) and Fe(II) irons are not greatly different from those respectively of $\mathrm{Fe_{(III)2}}$ and $\mathrm{Fe_{(III)1}}$ in eq 1 for Intermediate X, notably, $\mathbf{A} = 2.333\mathbf{A}_{\mathrm{Fe(III)}} - 1.333\mathbf{A}_{\mathrm{Fe(II)}}$. The upshot is that if intrinsic hyperfine tensors for nitrogen or protons are similar for Intermediate X, mixed-valent MMO, or semimet Hr, then the effective tensors and ENDOR frequencies also are similar.

coupling would arise with one maximal component along the iron-proton vector and two smaller perpendicular components. The maximum, intrinsic, largely dipolar contribution for a terminal water proton belonging to high spin d^5 Mn^{2+} [7a] or d^5 ferric heme[12] is about 7 MHz, and so one expects (using eq 1) to find a single, axial, maximal hyperfine coupling ($A_{||}$) of ~15 MHz for such a proton of water if the water were terminally ligated to $Fe_{(III)2}$ and of ~8 MHz if terminally ligated to $Fe_{(III)1}$. The implication is that the exchangeable proton(s) with couplings in the 18−23 MHz range are *not* terminal water protons, although the proton H,H′ with ~8 MHz coupling may be. A similar 8 MHz proton coupling was reported for mixed-valent MMO.[3b] (There appear to be features with couplings <4 MHz which may be exchangeable, but in this communication we focus on the unusual and better resolved large exchangeable coupling.)

A more strongly coupled terminal proton, conceivably a hydroxide proton, could provide an 18−23 MHz coupling. Such a coupling would still be axial with a maximum component in only one direction. Under conditions where the *g*-value anisotropy is well resolved, one might see good resolution of this large axial coupling only near one *g*-value. Such good resolution would be called good angle selection,[14,15] but the Intermediate X-Radical with its marginally resolved 0.5% *g* value anisotropy and its ~20 G EPR line width does not provide at X-band ideal conditions for high angle selection. With slight *g* anisotropy there is a greater likelihood of selected orientations that pass through an absolute extremum in hyperfine values.[14] It was encouraging to observe better resolution of the maximal hyperfine coupling at $g_{||}$; it was not surprising to see some remaining contribution of this maximum hyperfine coupling at $g_{\perp}$. This behavior can be explained by a hyperfine coupling with a large axial component close to $g_{||}$. Unfortunately, the small *g* anisotropy makes it difficult to determine the precise orientation of the hyperfine tensor to this strongly coupled, exchangeable proton.

The 18−23 MHz couplings of the exchangeable proton(s) are (at least superficially) reminiscent of the exchangeable proton couplings reported from mixed-valent MMO and Hr, where arguments[3b,c] were given that the responsible proton was attached to the hydroxo oxygen cross-bridge between the irons. As indicated in ref 13, a proton on the cross-bridging oxygen could have large hyperfine coupling in more than one direction and could in principle account for strongly coupled exchangeable features at both $g_{||}$ and $g_{\perp}$. The hyperfine tensor to a proton on the cross-bridging oxygen would be highly anisotropic and highly sensitive to its position between irons.

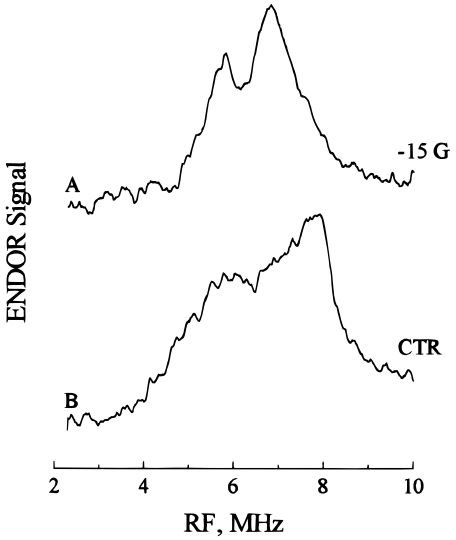

Figure 3. Spectra A and B were taken over a 2−10 MHz range with high field modulation to obtain details of spectra assigned to nitrogen. A. Spectrum from deuterated sample taken 15 G below the EPR line center under the following conditions: rf power = 1.2 W, microwave power ~ 0.5 μW, field modulation ~ 3 G ptp, rf noise broadening of approximately 100 KHz width, and 600 data accumulations of 10 s each at sweep rate of 0.8 MHz/s and system time constant 0.05 s. B. Spectrum from deuterated sample taken at the EPR line center under conditions identical to those in Figure 3A; the number of data accumulations was 106.

The nonexchangeable features, α, α′ with coupling of about 4.5 MHz, are most likely from protons on the carbons of histidine, the closest, nonexchangeable protons to the irons.[1] The intrinsic hyperfine coupling to such protons on proximal histidine of high spin ferric metmyoglobin is ~2 MHz,[12] and so after application of eq 1, such protons attached to $Fe_{(III)2}$ would be predicted to have an effective coupling of ~4.3 MHz.

Nitrogen ENDOR. The feature labeled N, which occurred below 10 MHz and was most obvious in the deuterated spectra shown in Figure 2A′,B′, had no proton partner. Detailed measurements of the feature labeled N revealed a sharp peak with ~1 MHz splitting as measured 15 G below the EPR line center (Figure 3A) and a ~3 MHz broad powder pattern (Figure 3B) at the line center. The sharp, split peak revealed some angle selection near $g_{||}$, and the broad peak near $g_{\perp}$ implied a powder pattern of orientations.[14,15]

First-order ENDOR expressions for a ^{14}N $I = 1$ nucleus are: the ν^+ branch at $\nu^+ = |1/2A^N + {}^{14}\nu + 3Q/2|$ and the ν^- branch at $\nu^- = |1/2A^N - {}^{14}\nu + 3Q/2|$, where A^N is the ^{14}N hyperfine coupling, $^{14}\nu$ is the nitrogen NMR frequency (~0.9 MHz at 3 KG), and Q is the quadrupole coupling. First-order theory is appropriate here because it is clear from the average position of the features that a large isotropic hyperfine coupling of order 10 MHz dominates. The upper (ν^+) and lower (ν^-) branches would be separated by twice the ^{14}N Larmor frequency ($2^{14}\nu \approx 2.0$ MHz). The lower branch ν^- is often very weak[15] for passage ENDOR, and we interpret the features in Figure 3A,B as arising from the ν^+ branch, occurring at $A/2 + {}^{14}\nu + 3Q/2$. There is ~1 MHz splitting of the feature measured near $g_{||}$. Near

(12) Mulks, C. F.; Scholes, C. P.; Dickinson, L. C.; Lapidot, A. *J. Am. Chem. Soc.* **1979**, *101*, 1645−1654.

(13) (a) For the potentially interesting case where the proton is attached to a cross-bridging oxygen, we took plausible coordinates for it from the structure of metR2 (ref 1b, Table 15), where the two irons are 3.3 Å distant and the iron to μ-oxygen distance is ~2.0 Å. The proton was taken 1 Å from the oxygen in a direction perpendicular to the Fe−Fe direction in the Fe−O−Fe plane so that the Fe-proton distance was 2.7 Å and the proton−Fe−Fe angle was 51°. The overall proton hyperfine tensor due to eq 1 was diagonalized after methods outlined in the "spin-coupled point-pair" approach of refs 13b,c. This approach had been first used to estimate dipolar hyperfine couplings for protons attached to oxygen cross-bridges in exchange-coupled manganese pairs. If the coupled radical spin was at the cross-bridging oxygen, then the resultant rhombic dipolar tensor had principle values of 20.6, −19.1, and −1.5 MHz. If only the spins on $Fe_{(III)1}$ and $Fe_{(III)2}$ were included in computing the tensor and there was no contribution from spin on the bridging oxygen, then the resultant rhombic dipolar tensor had principal values of 17.6, −21.9, and 4.3 MHz. In either case the two larger tensor values were ~20 MHz in magnitude and were in the Fe−O−Fe plane. (b) Tang, X.-S.; Sivaraja, M.; Dismukes, G. C. *J. Am. Chem. Soc.* **1993**, *115*, 2382−2389. (c) Kangulov, S.; Sivaraja, M.; Barynin, V.; Dismukes, G. C. *Biochemistry* **1993**, *32*, 4912−4924.

(14) Hurst, G. C.; Henderson, T. A.; Kreilick, R. W. *J. Am. Chem. Soc.* **1985**, *107*, 7294−7299.

(15) Hoffman, B. M.; DeRose, V. J.; Doan, P. E.; Gurbiel, R. J.; Housman, A. L. P.; Telser, J. Metalloenzyme Active Site Structure and Function by Multifrequency CW and Pulsed Electron Nuclear Double Resonance (ENDOR). In *EMR of Paramagnetic Molecules*; *Biological Magnetic Resonance 13*; Berliner, L. J., Reuben, J., Eds.; Plenum Press: New York, 1993; Chapter 4, pp 151−218.

a $g_{||}$ extreme hyperfine anisotropy would lead to a broadening rather than to a splitting in the frozen solution ^{14}N spectrum. The splitting of 1 MHz is too small to be Zeeman splitting. However, quadrupolar coupling permits such a splitting, whereby $|Q| \sim 0.3$ MHz accounts for a 1 MHz splitting ($=3|Q|$) in Figure 3A. Such a 0.3 MHz quadrupolar coupling for the proximal histidine nitrogen of metmyoglobin has been found along that direction which is mutually perpendicular to the imidazole N−Fe(III) bond and to the imidazole plane;[16] the implication here is that $g_{||}$ points near such a direction for the nitrogen being observed. At the central $g_{\perp}$ EPR line position one expects many orientations to contribute to the ENDOR pattern, which will be broadened by combined hyperfine and quadrupolar anisotropy. The two expected histidine components of quadrupolar interaction normal to the 0.3 MHz component would be ∼0.8 and ∼−1.1 MHz,[16] and they may well be the contributors to the broad ∼3 MHz splitting observed in Figure 3B at $g_{\perp}$.

The hyperfine coupling from the average of features in Figure 3A is 10.5 ± 0.5 MHz, and the hyperfine coupling for the average of features of Figure 3B is 11.0 ± 0.5 MHz. Since we observed no larger nitrogen couplings than these, the observed nitrogen histidine features is more likely from the histidine on $Fe_{(III)2}$. The intrinsic nitrogen hyperfine couplings from our data (by use of eq 1), would be in the range 4.9−5.1 MHz if the histidine nitrogen is located on $Fe_{(III)2}$ and 9.4−9.8 MHz if located on $Fe_{(III)1}$. In either case, these couplings are comparable to the intrinsic 8−11 MHz nitrogen hyperfine couplings of proximal histidine nitrogen from ferric metmyoglobin.[16] For the histidine nitrogen ligands to the Fe(III) of MMO and semimet Hr sulfide, the nitrogen couplings observed by X-band ENDOR were respectively 13.6 and 12.1 MHz.

(16) Scholes, C. P.; Lapidot, A.; Mascarenhas, R.; Inubushi, T.; Isaacson, R. A.; Feher, G. *J. Am. Chem. Soc.* **1982**, *104*, 2724−2735.

Conclusions

A large hyperfine coupling in the 18−23 MHz range was resolved from exchangeable protons of Intermediate X. This coupling was too large to be from terminally bound water. The magnitude of this coupling was better explained if the proton(s) causing it are on a strongly bound terminal hydroxide or on a cross-bridging oxygen between irons. The nitrogen ENDOR features must arise from iron-liganded histidine imidazole nitrogen, and the observed histidine is more likely the one bound to the iron [$Fe_{(III)2}$] of Intermediate X. The splitting of the nitrogen ENDOR signal at $g_{||}$ indicates a quadrupolar interaction like that observed from Fe-liganded imidazole nitrogen of metmyoglobin, implying that the direction corresponding to $g_{||} \approx 2.006$ is perpendicular to the Fe−N bond. Proton and nitrogen features observed here all have similarity to those features reported from ENDOR of mixed-valent methemerythrin and methane monoxygenase species.

Acknowledgment. We are grateful to Dr. D. Burdi, Dept. of Chemistry, MIT, for preparation of the ENDOR samples following his construction and expression of the R2-Y122F/Y356F mutant. We appreciate discussions with Professor JoAnne Stubbe. This work was supported by NIH Grant No. GM-35103.

IC951544I